a complex conformational epitope with contributions from both gp41 heptad repeat regions. Despite using the VH1-02 gene segment, known to contribute to some of the broadest neutralizing antibodies against HIV, members of these antibodies, termed group 76C antibodies, did not exhibit broad neutralization.

Methods. Our goal was to characterize the non-neutralizing functions of antibodies of group 76C, to assess targeting of the epitope in various clinical presentations, and to assess the development of these antibodies by comparison to their predicted common ancestor. Serum samples were obtained from HIV+ clinical groups: EC, LTNP, stable CD4 counts on therapy, and those off therapy.

Results. In antibody/serum competition assays, comparison to VRC01 which also uses VH1-02, showed that antibodies targeting the 76C group epitope were enriched in LTNPs. We then show recombinant antibodies of 76C members 6F5 and 6F11 both have robust ADCC activity, despite their sequence disparity. Sequence analysis predicted the common ancestor of this clonal group would utilize the germline non-mutated variable gene. We produced a recombinant ancestor Ab (76Canc) with a heavy chain utilizing the germline variable gene sequence paired to the 6F5 light chain. 76Canc binds HIV envelope constructs near the original group C epitope. 76Canc also shows comparable ADCC to 6F5 and 6F11 on both clade B and C constructs.

Common ancestor antibodies maintain function and these types of antibodies correlate to a non-progressive clinical state.

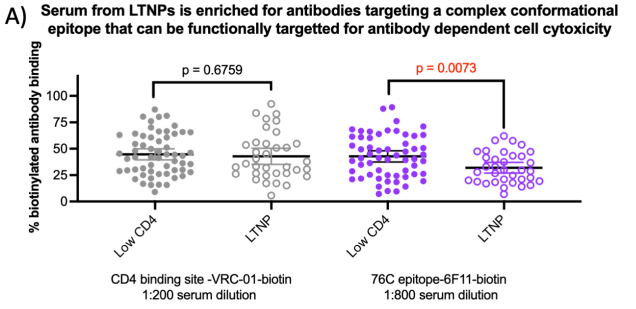

Serum from LTNPs compared to serum from a group of HIV infected with lower CD4 levels as a control for viral load were used to compete against biotinylated CD4 binding site (VRC01) and 76C Gp41 conformational epitope (6F11) targeting antibodies. Serum dilutions were chosen to align means near 50%. Means with 95% confidence intervals are shown.

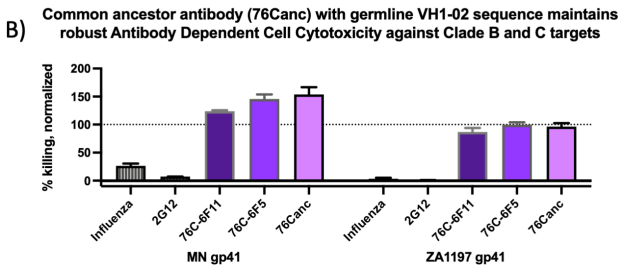

(A) Serum from long-term non-progressors (LTNPs) compared to serum from a group of HIV infected with lower CD4 levels as a control for viral load were used to compete against biotinylated CD4 binding site (VRC01) and 76C Gp41 conformational epitope (6F11) targeting antibodies. Serum dilutions were chosen to align means near 50%. Means with 95% confidence intervals are shown. (B) Monoclonal antibody 76Canc was created using the germline sequence of the heavy chain variable region with the CDR3 and light chain of 76C member. Antibody dependent cell cytotoxicity flow cytometric based assays were performed using gp41 proteins from clade B (MN) and clade C (ZA1197).

Conclusion. Certain antibodies present early on in infection may contribute to overall clinical course. Variable gene germline sequences that support functional activity against HIV could be targeted in vaccine regimens.

Disclosures. **All Authors**: No reported disclosures

1009. Biofilm Formation in *Acinetobacter Baumannii* Clinical Isolates

Elizabeth Nowak, M.D.[1]; Ekta Bansal, MD[2]; Anthony Baffoe-Bonnie, Medical Degree (M.D.)[3]; Nammalwar Sriranganathan, M.V.Sc., PhD., DACVM[4]; Thomas Kerkering, MD[5]; Jayasimha Rao, Ph.D.,MVPHA, FVPHA[6]; [1]Carilion Clinic, Roanoke, Virginia; [2]Virginia Tech Carilion School of Medicine, Roanoke, Virginia; [3]Carilion Clinic/VTCSOM, Roanoke, VA; [4]Virginia Polytechnic Institute and State University, Blacksburg, Virginia; [5]Virginia Tech Carilion School of Medicine, Carilion Clinic, Roanoke, VA; [6]Carilion Clinic/Virginia Tech Carilion School of Medicine, Roanoke, Virginia

Session: P-56. Microbial Pathogenesis

Background. Multidrug resistant *Acinetobacter baumannii* (MDR-Ab) is a Gram-negative bacterium known for causing severe nosocomial infections, attributed in part to its formation of biofilm. Siderophore is a virulence factor known to support biofilm formation by regulating iron availability. In this study, we screened 44 isolates of MDR-Ab from our Gram-negative repository to determine the strains that phenotypically form biofilm and produce siderophore. The results were compared to *Pseudomonas aeruginosa* PAO1, which produces both biofilm and siderophore.

Methods. Isolates were grown overnight in minimal M9 medium supplemented with casamino acids and hydroxyquinones at 37°C. Bacterial cells were normalized (to OD 600=0.01) and a standard diluted 10^{-3} tube was used in the study. A 96-well plate was inoculated with 100 microliters of each isolate in quadruplicates. This process was repeated in Tygon tubes with 50 microliters of each isolate in triplicates. The plate and Tygon tubes were incubated statically for 48 hours at 30°C and then stained with crystal violet. The contents were dissolved in 33% glacial acetic acid and analyzed by spectrophotometry to measure biofilm formation. Siderophore secretion was measured in supernatants with Chrome Azurol S (CAS) reagent and production was observed on CAS agar plates.

Results. High levels of biofilm formation were observed in 8 strains of MDR-Ab in the 96-well plate (3, 4, 9, 22, 61, 1010, 1012, 1022) and 6 strains in Tygon tubes (3, 4, 16, 66, 1002, 1010) (Fig. 1). There was minimal siderophore production in MDR-Ab isolates compared to PAO1 in both the 96-well plate and Tygon tubes (Fig. 2). Only 4 strains lacked siderophore production on CAS agar and were inversely negative for the secretion in medium.

Figure 1 Biofilm formation in a 96-well plate and Tygon tubes

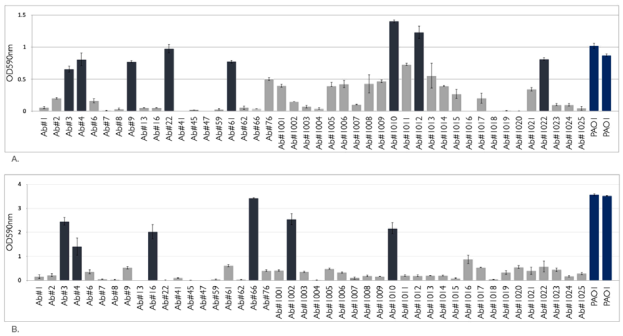

(A) High levels of biofilm formation were observed in MDR-Ab strain numbers 3, 4, 9, 22, 61, 1010, 1012, 1022 in the 96-well plate. (B) High levels of biofilm formation were observed in MDR-Ab strain numbers 3, 4, 16, 66, 1002, 1010 in Tygon tubes.

Figure 2 Degree of siderophore production in a 96-well plate and Tygon tubes

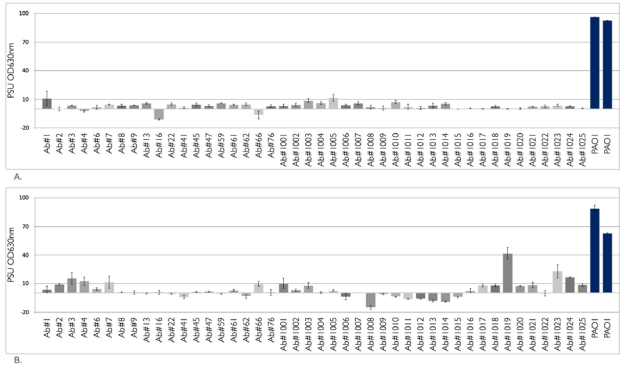

Siderophore production of MDR-Ab was limited compared to PAO1 after inoculation in a 96-well plate (A) and in Tygon tubes (B).

Conclusion. Many strains of MDR-Ab readily form biofilm. Overall siderophore production is lower in MDR-Ab compared to consistent production by PAO1, but this does not appear to affect MDR-Ab's ability to form biofilm. Unlike in PAO1, biofilm formation in MDR-Ab may occur independently of siderophore production. This research serves as a basis for understanding future MDR-Ab biofilm elimination in patient catheters and indwelling devices.

Disclosures. **All Authors**: No reported disclosures

1010. Cross-Species Translation of Correlates of Protection for COVID-19 Vaccine Candidates Using Quantitative Tools

Anna Largajolli, PhD[1]; Nele Plock, PhD[1]; Bhargava Kandala, PhD[2]; Akshita Chawla, PhD[2]; Seth H. Robey, PhD[2]; Kenny Watson, PhD[1]; Raj Thatavarti, MS[1]; Sheri Dubey, PhD[2]; S. Y. Amy Cheung, PhD[1]; Rik de Greef, MSc[1]; Jeffrey R. Sachs, PhD[2]; [1]Certara, Princeton, New Jersey; [2]Merck & Co., Inc., Kenilworth, New Jersey

Session: P-56. Microbial Pathogenesis

Background. Several COVID-19 vaccines have been authorized, and the need for rapid, further modification is anticipated. This work uses a Model-Based Meta-Analysis (MBMA) to relate, across species, immunogenicity to peak viral load (VL) after challenge and to clinical efficacy. Together with non-clinical and/or early clinical immunogenicity data (ECID), this enables prediction of a candidate vaccine's clinical efficacy. The goal of this work was to enable the accelerated development of vaccine candidates by supporting

Go/No-Go and study design decisions, and the resulting MBMA can be instrumental in decisions not to progress candidates to late stage development.

Methods. A literature review with pre-specified inclusion/exclusion criteria enabled creation of a database including nonclinical serum neutralizing titers (SN), peak VL after challenge with SARS-CoV-2 (VL), along with data from several clinical vaccine candidates. Rhesus Macaque (RM) and golden hamster (GH) were selected (due to availability and consistency of data) for MBMA modeling. For both RM and GH, peak post-challenge VL in lung and nasal tissues were used as surrogates for clinical disease and were related to pre-challenge SN via the MBMA. The VL predictions from the RM MBMA were scaled to incidence rates in humans, with a scaling factor between RM and human SN estimated using early Phase 3 efficacy data. This enabled clinical efficacy predictions based on ECID. To qualify the model's predictive power, efficacies of COVID-19 vaccine candidates were compared to those predicted from the MBMA and their respective Ph1/2 SN data. More recently available clinical data enable building a clinical MBMA; comparing this to the RM MBMA further supports SN as predictive.

Results. The MBMA analyses identified a sigmoidal decrease in VL (increasing protection) with increase in SN in all three species, with more SN needed (in both RM and GH) for protection in nasal swabs than in BAL (see figure). The comparison between predicted and reported clinical efficacies demonstrated the model's predictive power across vaccine platforms.

RM and GH MBMA Protection Models and Translational Prediction with Observed Efficacies

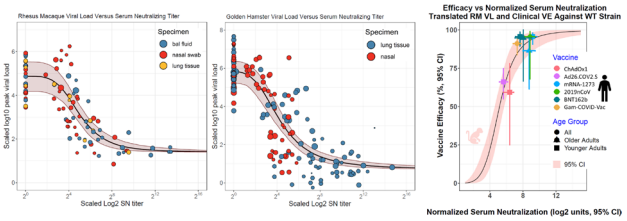

Sizes of circles indicate relative weight of the data in the respective quantitative model. Model and data visualizations have been harmonized (across tissue-types) separately for each of RM and GH using VACHER (Lommerse, et al., CPT:PSP, in press).

Conclusion. By quantifying adjustments needed between species and assays, translational MBMA can inform development decisions by using nonclinical SN and VL, and ECID to predict protection from COVID-19.

Disclosures. **Anna Largajolli, PhD**, **Certara** (Employee) **Nele Plock, PhD**, **Certara** (Employee, Shareholder)**Merck & Co., Inc.** (Independent Contractor) **Bhargava Kandala, PhD**, **Merck & Co., Inc.** (Employee, Shareholder) **Akshita Chawla, PhD**, **Merck & Co., Inc.** (Employee, Shareholder) **Seth H. Robey, PhD**, **Merck & Co., Inc.** (Employee, Shareholder) **Kenny Watson, PhD**, **Certara** (Employee, Shareholder) **Raj Thatavarti, MS**, **Certara** (Employee, Shareholder) **Sheri Dubey, PhD**, **Merck & Co., Inc.** (Employee, Shareholder) **S. Y. Amy Cheung, PhD**, **Certara** (Employee, Shareholder) **Rik de Greef, MSc**, **Certara** (Employee, Shareholder) **Jeffrey R. Sachs, PhD**, **Merck & Co., Inc.** (Employee, Shareholder)

1011. Geospatial Analysis of Antibiotic Susceptibility in Wisconsin

Laurel Legenza, PharmD, MS[1]; Kyle McNair, MS[1]; James P. Lacy, MS[1]; Song Gao, PhD[1]; Warren Rose, PharmD, MPH[1]; [1]University of Wisconsin-Madison, Madison, Wisconsin

Session: P-56. Microbial Pathogenesis

Background. The global threat of antimicrobial resistance (AMR) varies regionally. Regional differences may be related to socio-economic factors such as the Area Deprivation Index (ADI) score. Our hypothesis is that AMR spatial distribution is not random.

Methods. Patient level antibiotic susceptibility data was collected from three regionally distinct Wisconsin health systems (UW Health, Fort HealthCare, Marshfield Clinic Health System [MCHS]). Patient addresses were geocoded to coordinates and joined with US Census Block Groups. For each culture source, we included the initial *E. coli* isolate per patient per year with a patient address in Wisconsin. Percent susceptibility was calculated by block group. Spatial autocorrelation was determined by Global Moran's I, which quantifies the attribute being analyzed as spatially dispersed, randomly distributed, or clustered by a range of −1 to +1. Linear regression correlated ADI to susceptibility. Hot spot analysis identified blocks with statistically significant higher and lower susceptibility (Figure 1).

Figure 1. Geographic example of hot spot analysis and interpretation.

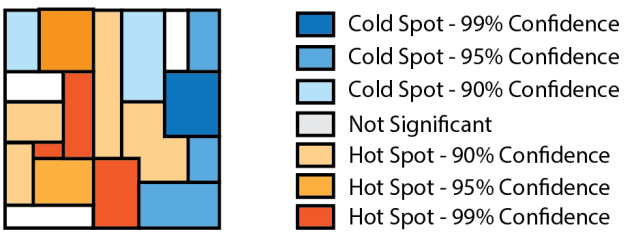

Results. The UW Health results included more urban areas, more block groups and greater isolate geographic density (n = 44,629 *E. coli*, 2009-2018), compared to Fort HealthCare (n = 6,065 isolates, 2012-2018) and MCHS (50,405 isolates, 2009-2018). A positive spatially clustered pattern was identified from the UW Health data for ciprofloxacin (Moran's I = 0.096, p = 0.005) and trimethoprim/sulfamethoxazole (TMP/SMX) susceptibility (Moran's I = 0.180, p < 0.001; Figures 2-3). Fort HealthCare and MCHS distribution was likely random for TMP/SMX and ciprofloxacin by Moran's I. Linear regression of ADI (scale 1-10, least to most disadvantaged) and susceptibility did not find significance, but susceptibility was lower in more disadvantaged block groups. At the local level, we identified hot and cold spots with 90%, 95%, and 99% confidence, with more hot spots in rural regions.

Figure 2. Results from Moran's Index analysis identifying geographically clustered ciprofloxacin susceptibility results.

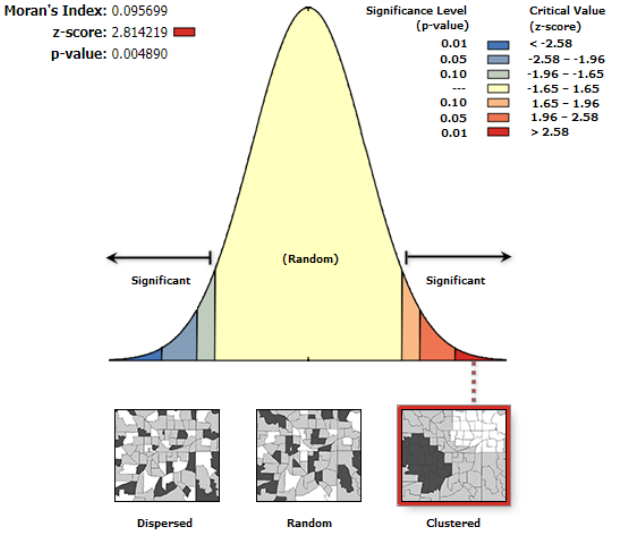

Given the z-score of 2.814219, there is a less than 1% likelihood that this clustered pattern could be the result of random chance.

Figure 3. Results from Moran's Index analysis identifying geographically clustered sulfamethoxazole/trimethoprim susceptibility results.

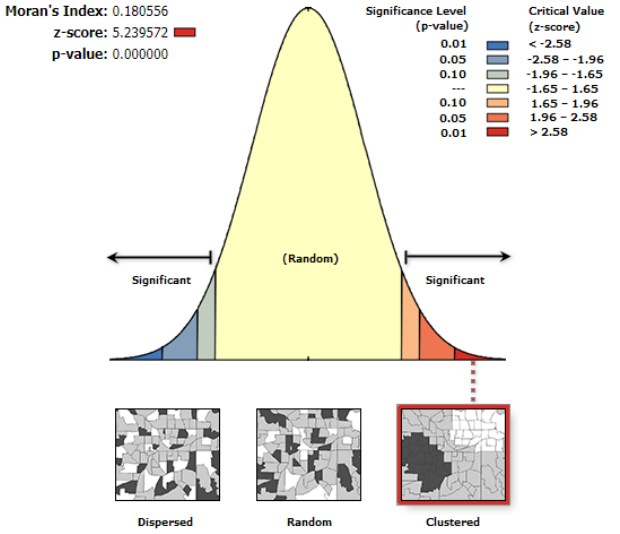

Given the z-score of 5.239572, there is a less than 1% likelihood that this clustered pattern could be the result of random chance.

Conclusion. Overall, Moran's I analysis is more able to identify a clustered pattern in urban versus rural areas. Yet, the local hot spot results indicate that variations in antibiotic susceptibility may be more common in rural areas. The results are limited to data from patients with access to the health systems included.

Disclosures. **Warren Rose, PharmD, MPH**, **Merck** (Grant/Research Support)**Paratek** (Grant/Research Support, Advisor or Review Panel member)